

Activation of FGF2-FGFR Signaling in the Castrated Mouse Prostate Stimulates the Proliferation of Basal Epithelial Cells¹

Manabu Kato,³ Kenichiro Ishii,⁴ Yoichi Iwamoto,³ Takeshi Sasaki,³ Hideki Kanda,³ Yasushi Yamada,³ Kiminobu Arima,³ Taizo Shiraishi,⁴ and Yoshiki Sugimura^{2,3}

³Department of Nephro-Urologic Surgery and Andrology, Mie University Graduate School of Medicine, Tsu, Mie, Japan

⁴Department of Oncologic Pathology, Mie University Graduate School of Medicine, Tsu, Mie, Japan

ABSTRACT

The prostate gland is unique in that it undergoes rapid regression following castration but regenerates completely once androgens are replaced. Residual ductal components play an important role in the regeneration of a fully functional prostate. In this study, to examine how androgen status affects prostate structure and components, we conducted histopathological studies of the involuted and regenerated mouse dorsolateral prostate (DLP). In the castrated mouse DLP, the number of luminal epithelial cells decreased in a time-dependent manner. On Day 14 postandrogen replacement, the number of luminal epithelial cells was completely restored to the baseline level. In contrast, the number of basal epithelial cells gradually increased in the castrated mouse prostate. The Ki67-labeling index of prostate basal epithelial cells was significantly increased after castration. The number of basal epithelial cells decreased to baseline after androgen replacement. After castration, mRNA expression levels of specific growth factors, such as *Fgf2*, *Fgf7*, *Hgf*, *Tgfa*, and *Tgfb*, were relatively abundant in whole mouse DLPs. In organ culture experiments, basal epithelial proliferation was recapitulated in the absence of dihydrotestosterone (DHT). The proliferation of basal epithelial cells in the absence of DHT was suppressed by treatment with an FGF receptor inhibitor (PD173074). Moreover, FGF2 treatment directly stimulated the proliferation of basal epithelial cells. Taken together, these data indicated that the FGF2-FGF receptor signal cascade in the prostate gland may be one of the pathways stimulating the proliferation of basal epithelial cells in the absence of androgens.

basal epithelial cells, castration, fibroblast growth factor 2, fibroblast growth factor receptor, growth factor, organ culture, prostate

INTRODUCTION

The prostate is a male accessory sex gland found only in mammals. Its main function is to produce a major fraction of the seminal fluid. Androgens are essential for the development, differentiation, growth, and function of the prostate [1]. In

adults, androgens act on androgen receptor (AR)-positive prostate epithelial cells to establish their functional differentiation into luminal secretory epithelial cells [2]. Androgens induce prostate epithelial cells to produce growth factors and cytokines that mediate stromal functions, including proliferation and differentiation [3, 4]. In the prostate stroma, androgens work to induce smooth muscle cells (SMCs) to produce a number of morphogens critical for maintaining differentiation and supporting glandular proliferation in the adult prostate [5]. Furthermore, under the influence of androgens, stromal cells produce mitogens that stimulate the proliferation of prostate epithelial cells [6]. Thus, these androgen-mediated paracrine effects maintain homeostasis in the adult prostate [7, 8]. Clinically, androgen deficiency contributes to the development of metabolic syndrome, late-onset hypogonadism, and infertility in men [9–11]. These reports indicate that androgens may also have an important regulatory role both outside of and within the male reproductive system.

Surgical or chemical castration induces marked regression of the prostate in several animal models, and castration-induced regression in the prostate has been well studied [12–15]. In the absence of androgen, prostate structural regression is mainly attributed to a functional decrease in the secretory activity of luminal epithelial cells and to a reduction in the number of luminal epithelial cells by apoptosis [16, 17]. Structural alterations also occur in the prostate stroma following castration and are characterized by replacement of SMCs by fibroblasts or myofibroblasts [18]. Evidence suggests that stromal remodeling following castration is accompanied by a functional transformation of the prostate stromal environment [19]. However, detailed evaluations of structural alterations occurring in the castrated prostate have produced controversial results. For example, English et al. [16] suggested a decrease in prostate secretory functions and reduction in prostate epithelial cells in the absence of androgen. In contrast, Shidaifat et al. [18] reported that during the substantial reorganization induced by castration, basal epithelial cells remained intact to form a continuous layer lining the atrophied prostate acini. Interestingly, this regression process after castration is reversible because androgen replacement completely regenerates the functional secretory prostate [14, 20–22]. The mechanisms of prostate regeneration may include the participation of prostate stem/progenitor cells that have a self-renewal ability [23, 24]. For example, a single transplanted stem cell is sufficient to regenerate the prostate in vivo [22]. Prostate regeneration likely also depends on specific growth factors, such as epidermal growth factor (EGF) and transforming growth factor α (TGF α), which are increased following androgen replacement [25]. It is likely that growth factors such as these recruit prostate stem/progenitor cells from out of a quiescent state [26]. These downstream pathways following androgen stimulation have not been fully elucidated and remain an area of great interest.

¹Supported by Grants-in-Aid from the Ministry of Education for Science and Culture of Japan (Nos. 22591764, 21592039, and 23791751) and the 2012 Mie Medical Research Foundation. Presented in part at the 107th American Urological Association Annual Meeting, 19–23, May 2012, Atlanta, Georgia.

²Correspondence: Yoshiki Sugimura, Department of Nephro-Urologic Surgery and Andrology, Mie University Graduate School of Medicine, 2–174 Edobashi, Tsu, Mie 514-8507, Japan.
E-mail: sugimura@clin.medic.mie-u.ac.jp

Received: 27 December 2012.
First decision: 6 February 2013.
Accepted: 8 August 2013.

© 2013 by the Society for the Study of Reproduction, Inc.
eISSN: 1529-7268 <http://www.biolreprod.org>
ISSN: 0006-3363

Specific growth factors are also increased in the setting of androgen withdrawal in the castrated mouse prostate [25, 27, 28]. In embryos, these growth factors stimulate the proliferation of epithelial cells and play an important role in prostate development and organogenesis [29, 30]. Transgenic mice overexpressing these growth factors exhibit proliferative abnormalities in the prostate. For example, overexpression of fibroblast growth factor 2 (FGF2) or FGF7 promotes hyperplasia of prostate epithelial cells [31, 32]. Moreover, engineered epithelial overexpression of IGF-1 causes hyperplastic prostate growth [33], and overexpression of TGF α increases the number of basal epithelial cells [34]. Given these observations, upregulation of growth factors in the absence of androgens may induce proliferative alterations, even in the regressed mouse prostate.

In this study, to examine how androgen status affects prostate structure, we first assessed the histopathological characteristics of involuted and regenerated mouse prostates. Next, we analyzed androgen status-dependent gene expression changes in growth factors in involuted and regenerated mouse prostates. Finally, to identify the specific signal cascade underlying the structural alterations observed in the castrated mouse prostate, we performed serum-free organ culture experiments using the adult mouse prostate.

MATERIALS AND METHODS

Animals

Male C57BL6/J mice were used for all the experiments. Mice were purchased from SLC Japan Inc. (Shizuoka, Japan). All the animals were housed individually in chip-bedded polyolefin cages in a room with controlled temperature (23°C \pm 1°C) and humidity (45%–65%) on a 12L: 12D photoperiod. Mice were provided with rodent food and tap water ad libitum. The Mie University's Committee on Animal Investigation approved the experimental protocol.

Reagents

Recombinant mouse FGF2 and mouse FGF7 were purchased from R&D Systems, Inc. (Minneapolis, MN) and QED Bioscience, Inc. (San Diego, CA), respectively. Dihydrotestosterone (DHT) was purchased from Sigma-Aldrich, Inc. (St. Louis, MO). The EGF receptor inhibitor (AG1478), hepatocyte growth factor (HGF) receptor inhibitor (c-Met kinase inhibitor III; 2-[6-{{R}}-1-[2,6-dichloro-3-fluorophenyl] ethoxy] quinolin-3-yl] cyclopropanecarboxamide), FGF receptor inhibitor (PD173074), and TGF β receptor I kinase inhibitor (LY364947) were purchased from Calbiochem, Inc. (San Diego, CA).

Antibodies

Mouse monoclonal p63 (clone 4A4) antibodies and rat monoclonal Ki67 (clone TEC-3) antibodies were purchased from Dako, Inc. (Copenhagen, Denmark). Mouse monoclonal E-cadherin antibodies (clone 36/E) were purchased from BD Transduction Laboratories (San Jose, CA).

Androgen Manipulation of Mice

Male C57BL6/J mice, ages 8–9 wk old (SLC Japan Inc. Sizuoka, Japan), were castrated through a scrotal incision under isoflurane-anesthesia. These mice were then sacrificed at 1, 3, 7, and 28 days after surgery. Each prostate was separated into anterior prostate, dorsolateral prostate (DLP), and ventral prostate (VP) lobes. For the androgen replacement experiment, mice were castrated as above and subcutaneously implanted with a 20 mg DHT pellet on Day 14 postcastration. At 1, 7, and 14 days after DHT pellet implantation, the mice were sacrificed, and the DLPs were collected. DHT pellets were made in our laboratory using a pellet press (Parr Instrument Company, Moline, IL). Castration and subcutaneous pellet implantation were performed under isoflurane anesthesia. DLPs were also collected from sham-treated control mice. Two lobes (right and left) collected from each castrated mouse were assigned to either histopathological analysis or RNA extraction. For histochemical analysis of the structural alterations of the mouse DLP after androgen manipulation, we used five mice for each time point. In gene

expression analysis of the mouse DLP after androgen manipulation, we used eight mice for each time point. Mouse DLPs were dissected at the end of the experiment. One lobe was fixed in formalin and processed in paraffin to confirm the immunohistochemistry, and the other lobe was immersed in RNAlater (Life Technologies, Carlsbad, CA) for mRNA extraction.

Histopathology and Immunohistochemistry

Serial sections (3 μ m thick) were cut on a Leica RM2125 rotary microtome (Leica Microsystems, Wetzlar, Germany) and mounted on glass slides. Sections were deparaffinized in Histoclear (National Diagnostic, Atlanta, GA) and hydrated in graded alcohol solutions and running tap water. For histopathology, standard hematoxylin and eosin staining was carried out. Next, immunohistochemical staining was performed with a Vectastain ABC Elite kit (Vector Laboratories, Inc., Burlingame, CA). After deparaffinization and hydration, endogenous peroxidase activity was blocked with 0.3% hydrogen peroxide in methanol for 20 min. After extensive washing in tap water, antigen retrieval was performed using Antigen Unmasking Solution (Vector Laboratories, Inc.) for p63, Ki67, and E-cadherin. Following a period of cooling and then rinsing in PBS, the sections were incubated in blocking solution for at least 30 min at room temperature. The sections were then incubated with primary antibodies at 4°C overnight. After incubation with primary antibodies, sections were incubated with the appropriate biotinylated secondary anti-goat, anti-mouse, or anti-rat immunoglobulin, which was included in the ABC Elite kit, for 30 min at room temperature. The antigen-antibody reaction was visualized using 3,3'-diaminobenzidine tetrahydrochloride as a substrate. Sections were counterstained with hematoxylin and examined by light microscopy. Anti-p63, anti-Ki67, and anti-E-cadherin antibodies were used at dilutions of 1:300, 1:300, and 1:3000, respectively.

RNA Extraction and cDNA Preparation

Total RNA was extracted using an RNeasy Mini Kit (Qiagen Inc., Valencia, CA) in accordance with the manufacturer's instructions. The RNA concentration was then determined spectrophotometrically. From 80 ng of total RNA, cDNA was reverse transcribed using a High Capacity RNA-to-cDNA Kit (Life Technologies).

Real-Time PCR Analysis

TaqMan quantitative PCR was performed with an Applied Biosystems StepOne Real-Time PCR system (Foster City, CA). TaqMan Gene Expression Assays for *Egf* (Mm00438696_m1), *Tgfa* (Mm00446232_m1), *Hgf* (Mm01135193_m1), *Igfl* (Mm00439560_m1), *Fgf2* (Mm00433287_m1), *Fgf7* (Mm00433291_m1), *Fgf10* (Mm00433275_m1), and *Tgfb* (Mm01178820_m1) were used with EagleTaq Master Mix containing ROX (Roche Diagnostics, Mannheim, Germany). All the data were analyzed with StepOne Software version 2.1 (Applied Biosystems) and normalized to *Gapdh* (Mm99999915_g1) mRNA levels.

Serum-Free Organ Culture of the Mouse Prostate

DLPs were cultured on Millicell CM filters (Millipore Corp., Billerica, MA) floating in medium in 6-well culture plates at 37.0°C in a humidified atmosphere with 5% CO₂ as previously reported [35]. The culture medium, phenol red-free Dulbecco modified Eagle medium (Invitrogen Corp., Carlsbad, CA) was supplemented with 10 mg/ml insulin (Sigma-Aldrich Co.), 10 mg/ml transferrin (Sigma-Aldrich Co.), 100 units/ml penicillin G, 100 mg/ml streptomycin, and 0.25 mg/ml amphotericin B (Invitrogen Corp.) [7, 36, 37]. Culture medium containing DHT (1 nM), 0.1% dimethylsulfoxide (control), or one of the growth factor receptor inhibitors (AG1478, c-Met kinase inhibitor III, PD173074, or LY364947) at a concentration of 10 nM was poured into each well and exchanged every other day. After 5 days of culture, the tissues were harvested, fixed in neutral buffered 10% formalin solution, and processed in paraffin for histopathological and immunohistochemical analyses. Three sequential *in vitro* organ culture experiments were conducted.

Image Analysis

For p63 index examination, each specimen was immunostained for p63 and digitally photographed (DP 70 camera, Olympus Corporation, Tokyo, Japan) through a system biomicroscope (BX50, Olympus Corporation, Tokyo, Japan) at 400 \times magnification. On each section, images were acquired from 10–15 representative sites. In the *in vivo* study, we evaluated the number of luminal epithelial cells and p63-positive basal epithelial cells in vertical sections of mouse prostate ducts at the same magnification (400 \times) for each time point.

Using the Win ROOF version 5.7 image analysis program (Mitani, Fukui, Japan), the numbers of p63-positive basal epithelial cells and luminal epithelial cells normally surrounded by an E-cadherin-positive membrane were counted individually. In this study, we defined luminal epithelial cells as p63-negative columnar cells with abundant cytoplasm and round nuclei located on the basement membrane surrounded by E-cadherin, whereas basal epithelial cells were defined as p63-positive cells, fusiform or triangular shaped, lying directly on the basement membrane with little cytoplasm and unclear nuclei. We determined the number of basal epithelial cells per 100 luminal epithelial cells on each image. For Ki67 index examination, each serial section was immunostained for p63, E-cadherin, and Ki67 and digitally photographed through a system biomicroscope at 400 \times magnification using the same device as was used for p63 index examination. On each section, images were acquired at 10–15 representative sites. We calculated the Ki67 index in luminal epithelial cells as the percentage of Ki67-positive luminal epithelial cells relative to the number of luminal epithelial cells surrounded by E-cadherin staining, exhibiting p63 negativity, and having morphological characteristics of luminal epithelial cells as described before. We calculated the Ki67 index in basal epithelial cells as the percentage of Ki67-positive basal epithelial cells relative to the number of p63-positive basal epithelial cells at the representative sites.

Statistical Analysis

Results were expressed as the means \pm SD. For analyses of in vivo mouse prostate structural alterations, gene expression, and in vitro organ culture with or without DHT, differences between the two groups were determined using Student *t*-tests with Bonferroni corrections. In these statistical analyses, differences with *P*-values of less than 0.05 divided by the number of statistical tests were considered statistically significant. For analysis of in vitro organ culture with one of the growth factor receptor inhibitors, differences between groups were determined using Dunnett multiple comparison. In these statistical analyses, differences with *P*-values less than 0.05 were considered statistically significant.

RESULTS

Alterations in the Structure and Components of the Mouse DLP after Castration and Subsequent Androgen Replacement

The adult mouse prostate showed structural regression and the loss of functional secretion after castration. Castration led to an 80% reduction in the wet weight of the mouse DLP (data not shown). Androgen replacement after castration resulted in a gradual regeneration of the prostate gland, that is, the precastration gland approximated Day 14 after androgen replacement.

After castration, the number of luminal epithelial cells lining the prostate ductal lumen decreased in a time-dependent manner, with significant differences apparent at 7 and 28 days postcastration in comparison to the control (Fig. 1, A–C and G). On Day 28 postcastration, only 30% of luminal epithelial cells remained (Fig. 1C). Androgen replacement gradually increased the number of luminal epithelial cells to baseline at Day 14 of treatment (Fig. 1G). The p63-positive basal epithelial cells were discontinuously attached to the basement membrane below the luminal epithelial cells on Day 1 postcastration (Fig. 1A). On Day 28 postcastration, however, p63-positive basal epithelial cells formed a continuous layer above the basement membrane surrounding the luminal epithelial cells in each duct (Fig. 1C). Two different image analyses confirmed that the number of p63-positive basal epithelial cells was gradually increased in a time-dependent manner with decreasing numbers of luminal epithelial cells and was significantly increased on Day 28 postcastration compared with the same time point in the control group (Fig. 1, G and H). In the castrated mouse prostate, the number of basal epithelial cells observed in vertical sections of mouse prostate ducts was increased in comparison to baseline (Fig. 1G). Additionally, the number of basal epithelial cells per 100 luminal epithelial cells increased following castration in a time-dependent manner (Fig. 1H). The number of basal epithelial cells also

returned to baseline following androgen replacement in a time-dependent manner (Fig. 1D–G). These findings indicated a relative increase in the number of basal epithelial cells.

To investigate whether the castration-induced relative increase in the number of basal epithelial cells in the mouse DLP was associated with the proliferation of basal epithelial cells, we examined the Ki67-labeling index of luminal and basal epithelial cells after castration. Data for the Ki67-labeling index of luminal and basal epithelial cells are summarized in Table 1. The Ki67 index of luminal epithelial cells in sham-operated mouse DLPs did not fluctuate at the various time points (Fig. 2, A and B, and Table 1). The Ki67 index of luminal epithelial cells in castrated mouse DLPs was decreased significantly and reflected a proliferative quiescence state from Day 14 after castration (Fig. 2, C and D, and Table 1). However, the Ki67 index of luminal epithelial cells in the mouse DLP was dramatically increased during prostate regrowth periods after androgen replacement (Fig. 2F and Table 1). From Day 17, that is, 3 days after androgen replacement, the Ki67-labeling index of luminal epithelial cells increased 20-fold, even on Day 28 (Fig. 2F and Table 1). As for basal epithelial cells, no proliferative state was observed in the sham-operated group (Fig. 2, A and B, and Table 1); however, the Ki67-labeling index of basal epithelial cells in the castrated mouse DLP was significantly increased from Day 3 after castration (Fig. 2, D and E, and Table 1). The Ki67-labeling index of basal epithelial cells increased 5-fold after castration and gradually decreased following androgen replacement (Table 1). On Day 28, the Ki67 index of basal epithelial cells was significantly decreased compared to that of the castrated group on Day 28 (Fig. 2F and Table 1).

Gene Expression Analysis of Growth Factors in the Mouse DLP after Castration and Subsequent Androgen Replacement

To investigate the effects of castration and subsequent androgen replacement on the gene expression of growth factors in the mouse DLP, gene expression was assessed with Taqman quantitative real-time PCR. After castration, the relative abundance of growth factor mRNAs for *Fgf2*, *Fgf7*, *Hgf*, *Tgfa*, and *Tgfb*, were observed to increase in whole mouse DLPs (Fig. 3, B, C, E, G, and H). The mRNA expression of *Egf* was decreased significantly after castration (Fig. 3A). No significant changes were found in the mRNA expression of *Fgf10* and *Igf1* (Fig. 3, D and F) after castration. Interestingly, after androgen replacement following castration, no changes occurred in the mRNA expression levels of *Fgf2*, *Fgf7*, *Hgf*, *Tgfa*, and *Tgfb*, all of which were relatively abundant in whole mouse DLPs after castration (Fig. 4, B, C, E, G, and H). Meanwhile, the mRNA expression of *Egf* and *Igf1* was relatively increased in whole mouse DLPs after androgen replacement following castration (Fig. 4, A and F).

Identification of the Signaling Cascade Associated with the Stimulation of Proliferation in Basal Epithelial Cells after Castration

To investigate whether castration-induced abundance of growth factors in whole mouse DLPs was involved in the proliferation of basal epithelial cells, we performed in vitro organ culture experiments using adult mouse DLPs. The consensus of discussions comparing mouse prostatic lobar anatomy with human prostatic zonal anatomy [38] suggests that the mouse DLP is likely homologous with the human peripheral zone, where prostate cancer generally occurs [39]; this has been reinforced by gene expression similarities between the mouse

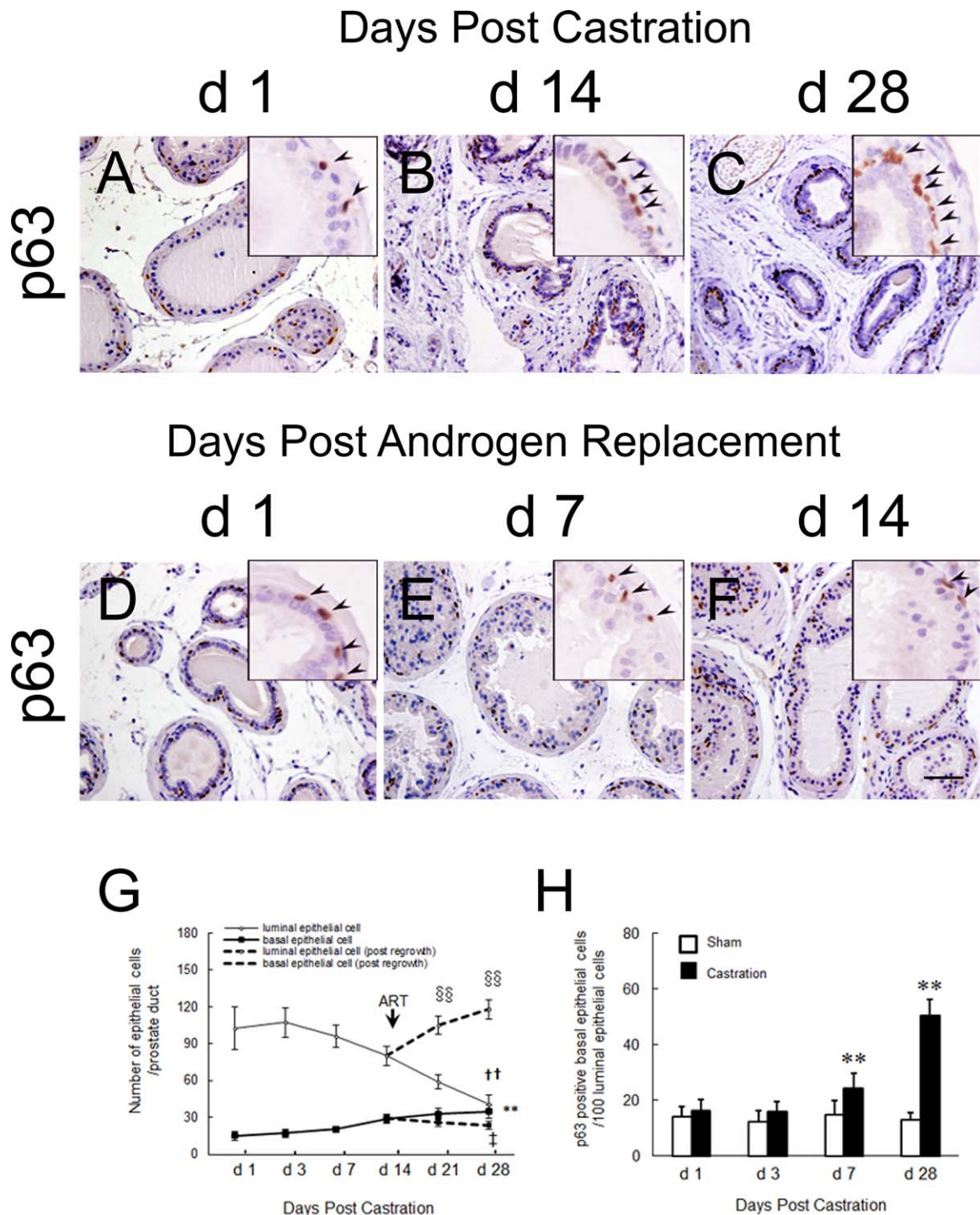


FIG. 1. Alterations in the structure and components of the mouse DLP after castration and subsequent androgen replacement. The p63-stained sections from the adult castrated mouse DLP on Days 1, 14, and 28 postcastration are shown in **A**, **B**, and **C**, respectively. The p63-stained sections from the regenerated (postandrogen replacement) mouse DLP on Days 1, 7, and 14 are shown in **D**, **E**, and **F**, respectively. **G**) Effects of androgen status on the number of prostate epithelial cells per DLP duct. \circ indicates luminal epithelial cells, \blacksquare indicates basal epithelial cells, and --- indicates regenerated mouse DLP epithelial cells. ART, androgen replacement treatment. **H**) Effects of androgen status on the number of p63-positive basal epithelial cells per 100 luminal epithelial cells. The number of basal epithelial cells per 100 luminal cells was evaluated in the castrated mouse DLP on Days 1, 3, 7, and 28. Values represent the means \pm SD for at least 10 DLP ducts. $**P < 0.01$ and $^{\dagger\dagger}P < 0.01$ versus the control (sham) group at each time point; $^{\ddagger}P < 0.05$ and $^{\S\S}P < 0.01$ versus the castration group at each time point. $*$, ‡ and § were used to denote statistically significant differences among the basal epithelial cell groups and luminal epithelial cell groups, respectively. Inserts shows images with a magnification $\times 400$, arrowheads indicate basal epithelial cells. Bar = 100 μm , magnification $\times 200$.

DLP and the human peripheral zone [40]. In the serum-free organ culture experiments, prostate epithelial and stromal cells were cultured simultaneously, maintaining epithelial-stromal interactions [41], allowing the effects of humoral factors, such as

steroid hormones and growth factors, to be evaluated directly [35]. First, we examined whether proliferation of the basal epithelium, which was observed after castration in vivo, was recapitulated using organ culture experiments in the absence of

TABLE 1. Changes in the Ki67-labeling index in mouse DLP epithelia after castration and castration-androgen replacement.

Day	Luminal epithelia			Basal epithelia		
	Sham (%)	Castration (%)	Androgen replacement (%)	Sham (%)	Castration (%)	Androgen replacement (%)
Day 1	3.4 ± 2.7	1.3 ± 1.5		0 ± 0	1.1 ± 2.3	
Day 3	3.1 ± 1.4	0.4 ± 0.7**		0 ± 0	5.0 ± 2.8**	
Day 7	1.9 ± 1.4	0.7 ± 0.8		0 ± 0	6.4 ± 2.6**	
Day 14	2.4 ± 3.2	0 ± 0		0 ± 0	4.7 ± 2.7**	
Day 17		0 ± 0	19.6 ± 6.1 [‡]		3.7 ± 3.1	7.5 ± 6.0
Day 21		0.30 ± 0.8	8.2 ± 3.5 [‡]		6.7 ± 2.6	2.6 ± 3.0
Day 28		0 ± 0	8.0 ± 3.1 [‡]		4.9 ± 5.2	0.9 ± 1.9 [†]

**P < 0.01 versus the control (sham) group; [†]P < 0.05, [‡]P < 0.01 versus the castration group.

androgen. In the control medium with DHT (1 nM), the luminal epithelial cells were tall and columnar with basally located nuclei, the discontinuous layer of basal epithelial cells was preserved, and the secretory functions were maintained (Fig. 5A). In the absence of DHT, the luminal epithelial cells became cuboidal or lowly columnar, similar to those in the castrated adult male mouse (Fig. 5B). The number of basal epithelial cells was significantly increased without DHT in a time-dependent manner (Fig. 5G). Furthermore, the Ki67 index of basal epithelial cells was significantly increased without DHT (Fig. 6, A and B, and Table 2). Thus, these findings indicate that this ex vivo prostate culture model accurately simulated the structural alterations of the castrated mouse DLP.

Next, we performed organ culture experiments with growth factor receptor inhibitors to examine whether the observed basal epithelial proliferation was caused by castration-induced abundance of growth factors in whole mouse DLPs. We conducted serum-free organ cultures of mouse DLPs without DHT but with one of each of the following growth factor receptor inhibitors (10 nM): FGF receptor inhibitor (PD173074), EGF/TGF α receptor inhibitor (AG1478), HGF receptor inhibitor (c-Met kinase inhibitor), or TGF β receptor 1 inhibitor (LY364947) (Fig. 5C–F). PD173074 significantly suppressed the increase in basal epithelial cells in comparison to the control (Fig. 5, C and H). The suppressive effect of PD173074 was observed in a dose-dependent manner (data not shown). However, in DLPs cultured with other receptor inhibitors, no suppression of basal epithelial proliferation was observed (Fig. 5H). Ki67-positive basal epithelial cells were also observed in cultured mouse DLPs (Fig. 6). Among the growth factor receptor inhibitors investigated, PD173074 suppressed the increase in the Ki67 index in basal epithelial cells without DHT (Fig. 6C and Table 2).

Among the FGFs investigated, the mRNA expression levels of *Fgf2* and *Fgf7* were relatively abundant in whole mouse DLPs after castration (Fig. 3, B and C). Thus, we conducted serum-free organ culture experiments with either FGF2 or FGF7 to examine which FGF directly affected the proliferation of basal epithelial cells. The number of basal epithelial cells was significantly increased by FGF2, but not by FGF7, when compared to the control (Fig. 7C–E). The Ki67 index of basal epithelial cells was significantly increased in FGF2-treated mouse DLPs (Fig. 8C and Table 3).

DISCUSSION

In this study, we demonstrated that the growth of basal epithelial cells was inversely dependent on androgen status. Androgen replacement reversed this increase. After castration, the mRNA expression of growth factors, such as *Fgf2*, *Fgf7*, *Hgf*, *Tgfa*, and *Tgfb*, was relatively increased in whole mouse DLPs. Castration-dependent changes in the expression of growth factor mRNAs in prostates have been reported previously [25]. Although previous reports have focused on the fluctuation of growth factors in the prostate after castration, the essential roles of those growth factors in the prostate after castration have not been well understood. Using an in vitro organ culture system, we demonstrated that an FGFR inhibitor suppressed the proliferation of basal cells following androgen withdrawal. Furthermore, the proliferation of basal epithelial cells was attributable to a direct effect of FGF2. This suggested that activation of the FGF2-FGFR signaling cascade in the castrated mouse DLP stimulated the proliferation of basal epithelial cells.

FGF2 is important in prostate growth [42]. FGF2 acts as a powerful mitogen, stimulating prostate epithelial cell differen-

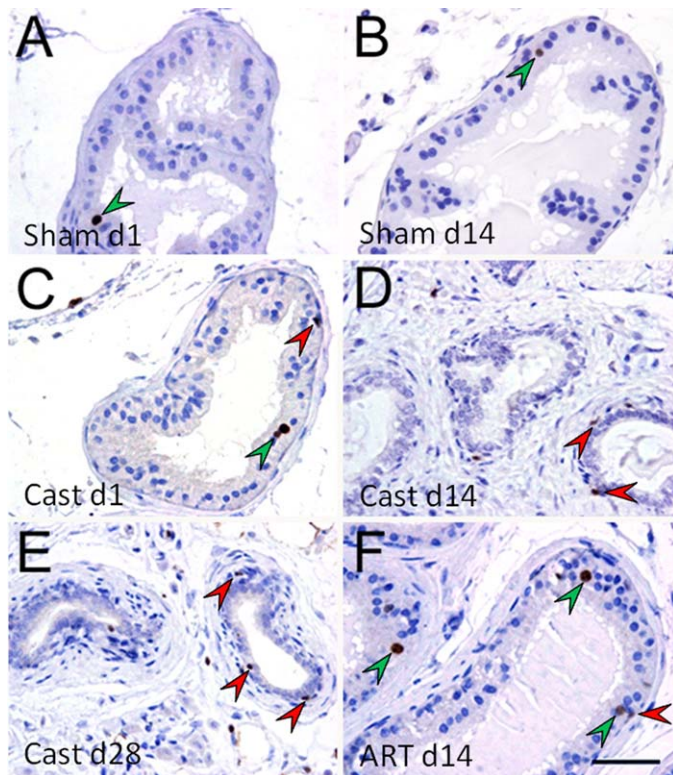


FIG. 2. Changes in the Ki67-labeling index in mouse DLP epithelia after castration and subsequent androgen replacement. Ki67-stained sections from the adult sham operated mouse DLP on Days 1 and 14 postsham operation are shown in A and B, respectively. Ki67-stained sections from the adult castrated mouse DLP on Days 1, 14, and 28 postcastration are shown in C, D, and E, respectively. Ki67-stained sections from the regenerated (postandrogen replacement) mouse DLP on Day 28 are shown in F. Green arrowheads indicate Ki67-positive luminal epithelial cells. Red arrowheads indicate Ki67-positive basal epithelial cells. Bar = 50 μ m, magnification \times 400.

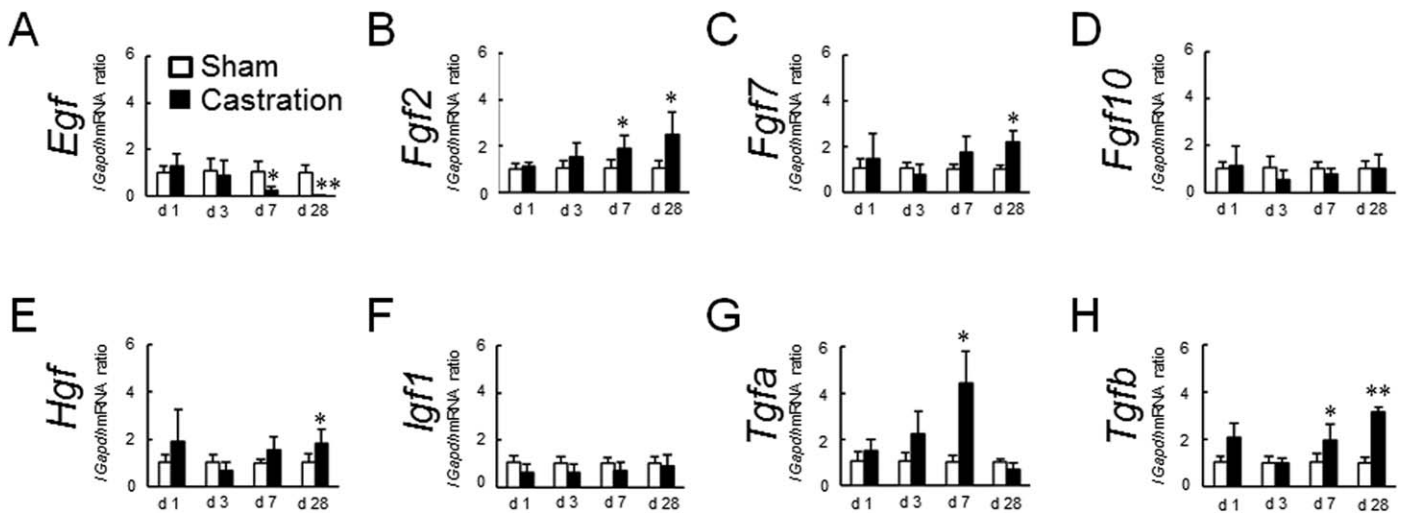


FIG. 3. Gene expression analysis of growth factors in the mouse DLP after castration. The relative mRNA expression levels of growth factors, including *Egf* (A), *Fgf2* (B), *Fgf7* (C), *Fgf10* (D), *Hgf* (E), *Igf1* (F), *Tgfa* (G), and *Tgfb* (H), were determined in control (open bar) and castrated (closed bar) mouse DLPs on Days 1, 3, 7, and 28 after castration. All the data were normalized to *Gapdh* mRNA levels; * $P < 0.05$ and ** $P < 0.01$ versus the control (sham) group at each time point.

tiation and proliferation as well as angiogenesis [43]. The mitogenic role of FGF2 in the prostate stroma is also significant [44]. In contrast, mRNA expression of FGF2 in the cultured embryonic rat urogenital sinus mesenchyme is downregulated in the absence of androgens [45]. These data and our results suggest that regulation of FGF2 expression might be dependent on the stage of prostatic development, that is, the embryonic versus the differentiated adult prostate. The signal cascade of FGFs has recently been well studied. FGF2 binds FGFR1 with high affinity [46], leading to the activation of a number of signaling molecules, including the RAS/RAF/MAPK (mitogen-activated protein kinase) pathway [47], the PI3K/AKT/mTOR pathway [48], and other signaling molecules, thereby inducing cell growth, differentiation, survival, and apoptosis. FGFR1 is primarily located in the prostatic stroma and some basal epithelial cells [49, 50], and FGF2 has been reported to be mainly produced in stromal cells of the prostate [51]. The expression levels of both FGF2 and FGFR1

are increased in the rat prostate following castration [25]. These data and our results support the idea that FGF2 may induce functionally active FGFR1 to stimulate the increase in basal epithelial cells. Our data showed that FGF2 treatment increased the number of p63-positive basal cells; the number of luminal cells was also increased as compared to FGF7 treatment. However, our organ culture system may have some limitations. Although the organ culture system could recapitulate the behavior of basal epithelial cells following castration, it could not exactly recapitulate the apoptotic loss and decrease of luminal epithelial cells observed in the in vivo castrated mouse prostate. We suggest that this is due to differences in the ingredients of the culture medium, such as insulin and transferrin, which strongly maintain mouse prostate tissue removed from the host mouse body.

On the other hand, previous reports have demonstrated biological features of mouse models that overexpressed FGF2, FGF7, IGF-I, or TGF α [31–34]. Hyperplastic luminal epithelial

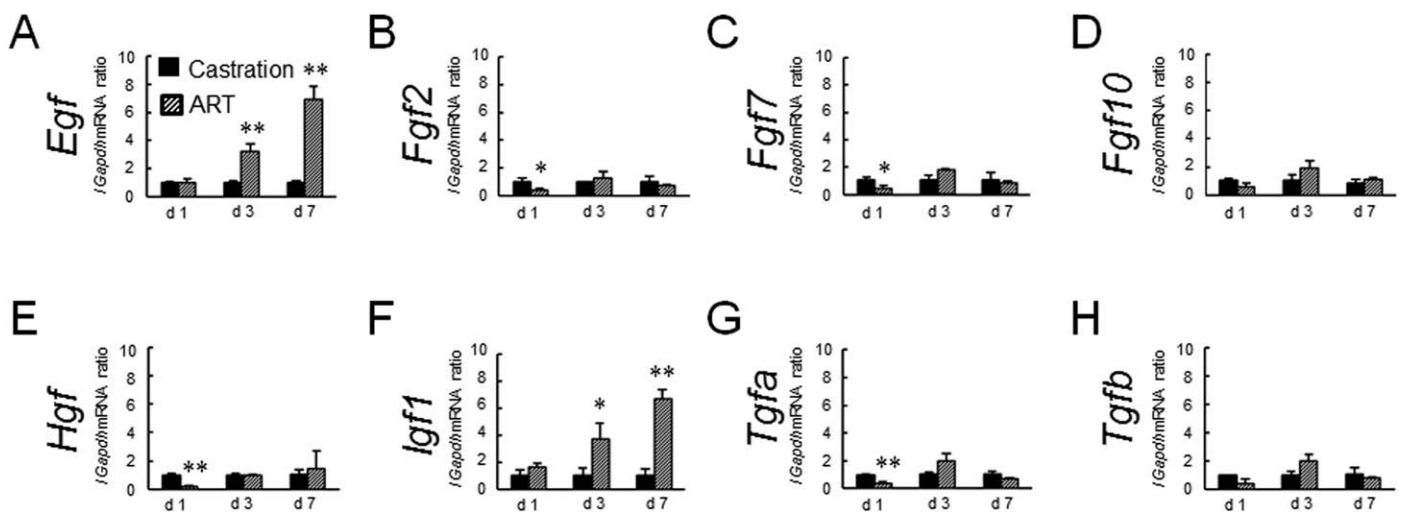


FIG. 4. Gene expression analysis of growth factors in the mouse DLP after castration and subsequent androgen replacement. The relative mRNA expression levels of growth factors, including *Egf* (A), *Fgf2* (B), *Fgf7* (C), *Fgf10* (D), *Hgf* (E), *Igf1* (F), *Tgfa* (G), and *Tgfb* (H), were determined in the castrated mouse DLP (closed bar) and in the mouse DLP on Days 1, 3, and 7 after androgen replacement followed by castration (stripped bar). All the data were normalized to *Gapdh* mRNA levels; * $P < 0.05$ and ** $P < 0.01$ versus the castration group at each time point.

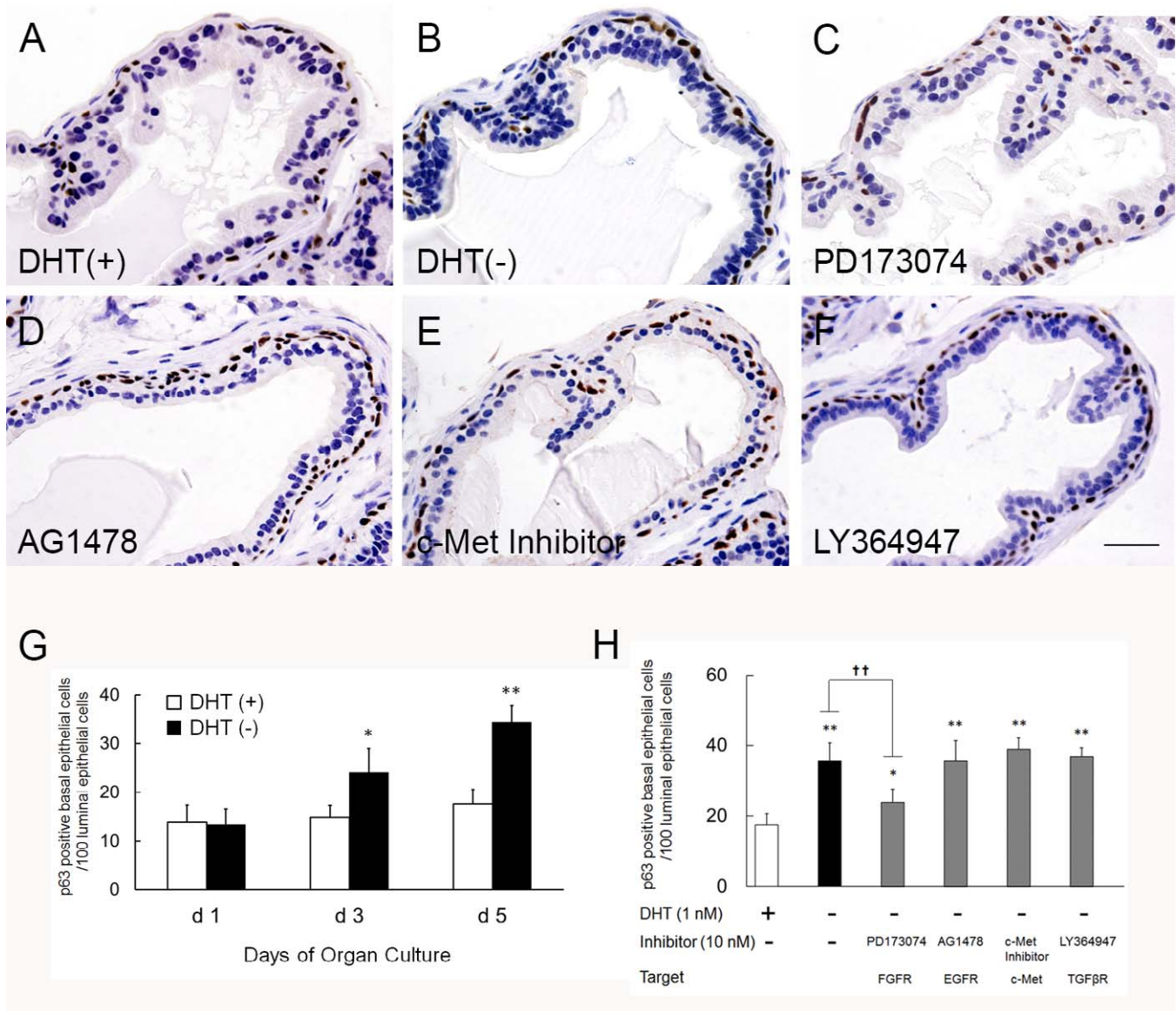


FIG. 5. Alterations in the structure and components of the cultured mouse DLP without androgen. The p63-stained sections from the adult mouse DLP cultured for 5 days with DHT (1 nM) or without DHT are shown in **A** and **B**, respectively. **C-F** The p63-stained sections from the adult mouse DLP were treated for 5 days with one of the following growth factor receptor inhibitors (10 nM): PD173074 (**C**), AG1478 (**D**), c-Met kinase inhibitor III (**E**), or LY364947 (**F**). Bar = 50 μ m, magnification \times 400. **G** The number of p63-positive basal epithelial cells per 100 luminal epithelial cells was evaluated in the mouse DLP cultured with or without DHT (1 nM) in organ culture experiments on Days 1, 3, and 5. * $P < 0.05$ and ** $P < 0.01$ versus with DHT (1 nM) at each time point. **H** The number of p63-positive basal epithelial cells per 100 luminal epithelial cells was evaluated in mouse DLPs cultured with DHT (1 nM) or one of the following growth factor receptor inhibitors (10 nM): PD173074, AG1478, c-Met kinase inhibitor III, or LY364947. †† $P < 0.01$ versus without DHT.

cells have been observed in the dorsal lobe of FGF2-overexpressing mouse prostates [31]. However, Ki67 staining for luminal epithelial cells revealed that few Ki67-positive cells were present in this mouse model [31]. Likewise, histological hyperplastic changes and the neuroendocrine phenotype were observed in epithelial cells of the mouse prostate following forced FGF7 expression [32]. However, evaluation of proliferation, such as determination of the Ki67 index, was not conducted in that study. Hyperplastic changes in epithelial cells have also been observed in the mouse prostate following forced IGF-1 expression without the evaluation of epithelial proliferation using a specific marker, such as Ki67 staining [33]. Yoshio et al. [34] demonstrated that the number of basal epithelial cells in the prostate of TGF α -overexpressing mice increased. They have also shown that proliferation of epithelial

cells in TGF α -overexpressing mouse DLPs was not observed by analysis of the Ki67-labeling index [34]. These models were not extensively evaluated in terms of histological alterations in the mouse prostate. Although these reports showed that the Ki67 index in the prostate was not significantly changed, immunohistochemistry was not performed to identify and precisely examine the proliferation index of each mouse prostate luminal or basal epithelial cells. Thus, our data are novel and provide important insights into the proliferation of these crucial subsets of cells.

Prostatic basal epithelial cells are critical for maintaining ductal integrity and regulate both the survival and apoptosis of luminal epithelial cells [52, 53]. Prostate progenitor and stem cells have been identified within the basal compartment [53]. These basal epithelial cells, which have stem-like activity, are

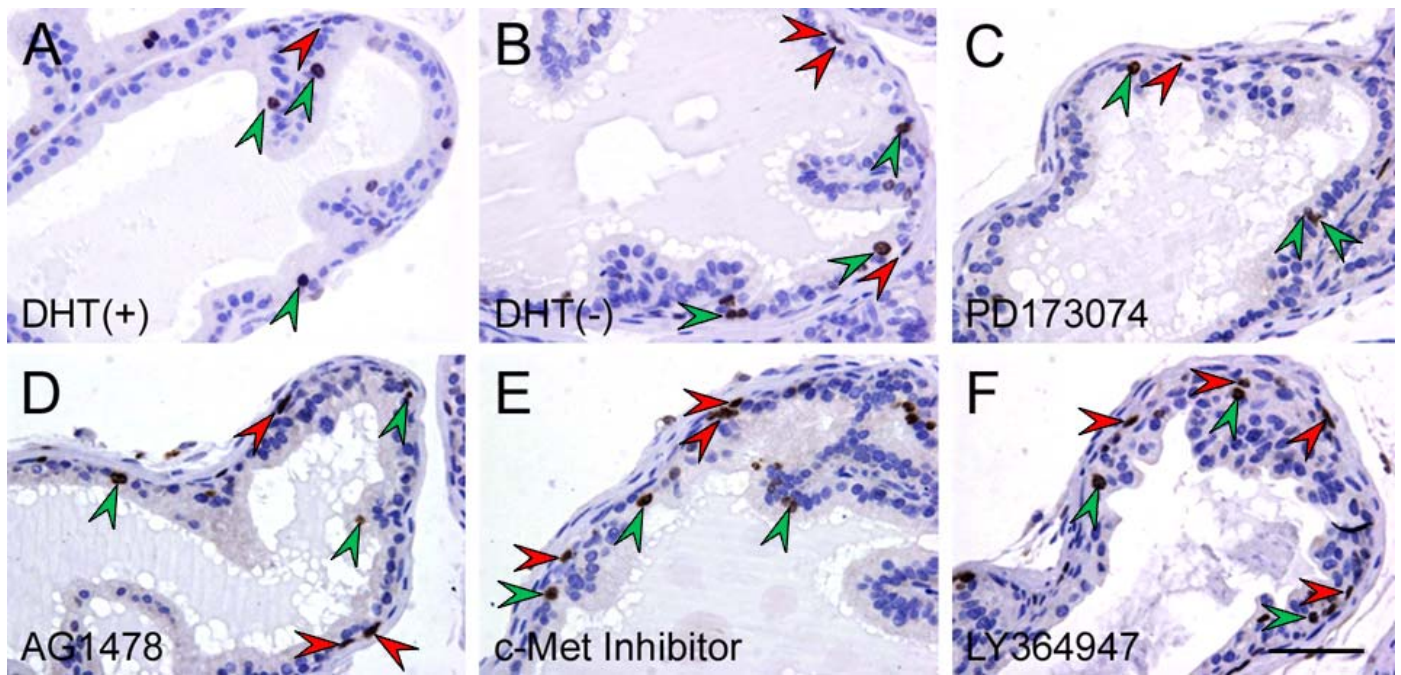


FIG. 6. Effects of growth factor receptor inhibitors on the Ki67-labeling index in basal epithelial cells. Ki67-stained sections from adult mouse DLPs cultured for 5 days with DHT (1 nM) or without DHT are shown in **A** and **B**, respectively. **C–F** The p63-stained sections from adult mouse DLPs were treated for 5 days with one of the following growth factor receptor inhibitors (10 nM): PD173074 (**C**), AG1478 (**D**), c-Met kinase inhibitor III (**E**), or LY364947 (**F**). Green arrowheads indicate Ki67-positive luminal epithelial cells, and red arrowheads indicate Ki67-positive basal epithelial cells. Bar = 50 μ m, magnification $\times 400$.

presumably located in a niche-like site within the basal epithelial layer [54]. An increase in these cells is referred to as basal cell hyperplasia, which is defined as the presence of basal cell proliferation composed of two or more layers of small cells with scant cytoplasm, and presents as glands or solid nests [55]. Basal cell hyperplasia is occasionally a component of untreated benign prostatic hyperplasia, which arises in the transition zone in the human prostate [55–57].

The androgen concentration in the hypertrophic human prostate decreases significantly with age [58]. In DLPs of senescence-accelerated mice that are androgen deficient, stromal fibrosis, the presence of atypical glandular epithelial cells, and cribriform glandular deformities were observed as age-related alterations [59]. In the canine prostate, the effects of androgen ablation on basal epithelial cells and luminal epithelial cells are associated with a marked increase in the stromal fibromuscular compartment, which demonstrates impaired differentiation [18]. The age-related expansion of proliferating acinar basal epithelial cell populations, mediated by sex steroids, is a key factor in the pathogenesis of canine prostatic hyperplasia [60]. In the human prostate, androgen ablation by antiandrogen therapy for prostate cancer patients

results in basal cell hyperplasia with variable focal squamous metaplasia localized diffusely throughout the benign prostate tissue [61]. These findings and our results indicate that aberrant proliferation of the prostate epithelial cells may be related to the concentration of androgen in the prostate.

Several studies have reported that androgen ablation leads to the death of secretory epithelial cells, while basal cells, the AR-negative population, survive [18]. Our results also showed that the number of basal epithelial cells was affected by changes in androgen status. Interestingly, the number of basal epithelial cells was increased in the absence of androgen and returned to baseline following androgen replacement. We propose that these proliferative alterations observed in the regressed prostate might compensate for the loss of luminal epithelial cells in order to maintain residual ductal components. Androgen replacement after castration drives the complete regeneration of the gland, which is derived entirely through the proliferation and differentiation of surviving cells, including basal epithelial cells [62, 63]. Thereby, these findings and our results support the idea that the decrease in basal epithelial cells observed in the regenerated mouse prostate following androgen replacement may result from the recruitment of these cells into luminal epithelial cells. It is also possible that the relative abundance of growth factors in whole mouse DLPs and the increased number of basal epithelial cells after castration confer an advantage for prostate regeneration should androgen replacement occur.

Using rat VPs, English et al. [16] reported that both luminal and basal epithelial cells decreased with androgen withdrawal to different levels. In this study, however, we found that prostate basal epithelial cells behaved differently according to androgen status. The proliferation of basal epithelial cells was inversely correlated to androgen level. In addition, we presented evidence that androgen ablation by surgical castration augmented *Fgf2* mRNA levels in whole mouse DLPs, which led to aberrant activation of the FGF2-FGFR signaling

TABLE 2. Effects of growth factor inhibitors on the Ki67-labeling index in basal epithelial cells.

Growth factor inhibitor	Ki67-labeling index (%)
1 nM DHT	9.2 \pm 2.0
Without DHT	12.8 \pm 2.0**
PD173074	8.0 \pm 1.1 [†]
AG1478	15.7 \pm 4.8**
c-Met inhibitor	12.2 \pm 3.6**
LY36497	13.5 \pm 4.4**

** $P < 0.01$ versus groups with DHT.

[†] $P < 0.01$ versus groups without DHT.

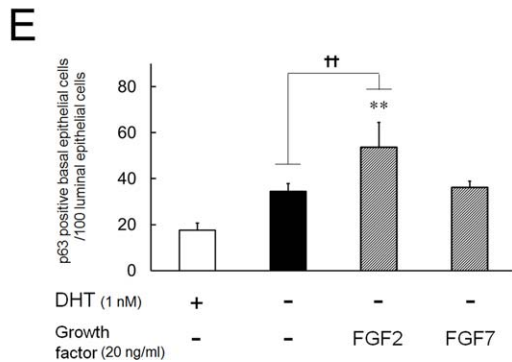
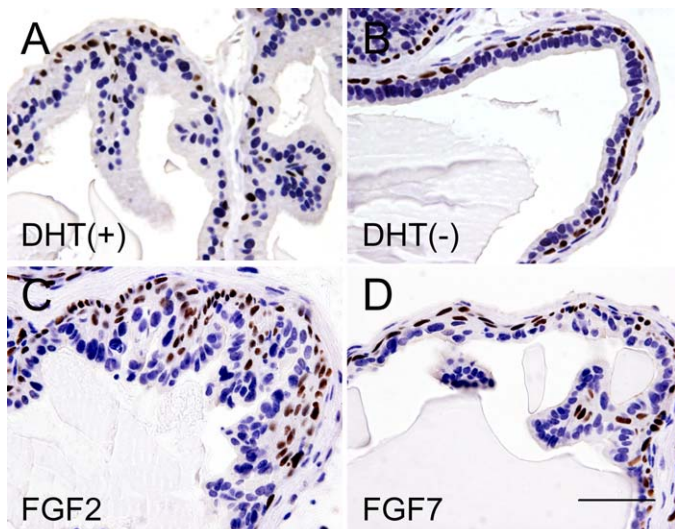


FIG. 7. Direct effects of FGFs on structural changes in the mouse DLP. Images of p63 staining in untreated tissues with or without DHT are shown in **A** and **B**, respectively. The p63-stained sections from adult mouse DLPs cultured for 5 days with FGF2 (20 ng/ml) or FGF7 (20 ng/ml) are shown in **C** and **D**, respectively. Bar = 50 μ m, magnification \times 400. **E**) The number of p63-positive basal epithelial cells per 100 luminal epithelial cells was evaluated in the mouse DLP cultured with DHT (1 nM), FGF2 (20 ng/ml), or FGF7 (20 ng/ml) at Day 5. ** $P < 0.01$ versus with DHT, and $\dagger\dagger P < 0.01$ versus without DHT.

cascade and subsequent proliferation of basal epithelial cells. Our results suggested that androgens may suppress the activation of FGF2-FGFR signaling, which induces proliferative alterations in the prostate. Further studies are needed to elucidate the molecular aspects of the androgenic effects on basal epithelial cells and stromal-epithelial interactions. This may eventually increase our understanding of the homeostatic biology of the prostate and the mechanisms of prostate disease.

TABLE 3. Direct effects of FGFs on the Ki67-labeling index in basal epithelial cells.

Fibroblast growth factors	Ki67-labeling index (%)
1 nM DHT	9.2 \pm 2.0
Without DHT	12.8 \pm 2.1*
20 ng/ml FGF2	22.2 \pm 8.7** \dagger
20 ng/ml FGF7	12.2 \pm 2.2

* $P < 0.05$, ** $P < 0.01$ versus groups with DHT.
 $\dagger P < 0.01$ versus groups without DHT.

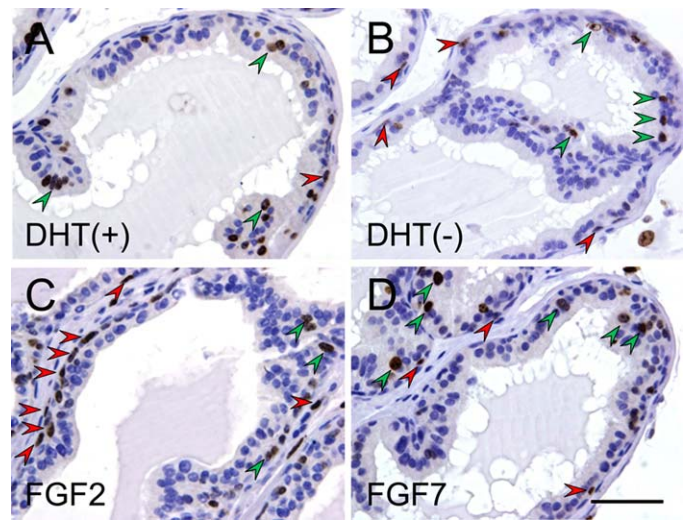


FIG. 8. Direct effect of FGFs on the Ki67-labeling index in basal epithelial cells. Images of Ki67 staining in untreated tissues with or without DHT for 5 days are shown in **A** and **B**, respectively. Ki67-stained sections from adult mouse DLPs cultured for 5 days with FGF2 (20 ng/ml) or FGF7 (20 ng/ml) are shown in **C** and **D**, respectively. Green arrowheads indicate Ki67-positive luminal epithelial cells, and red arrowheads indicate Ki67-positive basal epithelial cells. Bar = 50 μ m, magnification \times 400.

ACKNOWLEDGMENT

We thank Mrs. Yumi Yoshikawa and Mr. Ryo Nimura for their technical support. We are also grateful to Dr. Tomomi Yamada, Department of the Translational Medical Science, Mie University Graduate School of Medicine, for help with the statistical analysis.

REFERENCES

- Cunha GR, Donjacour AA, Cooke PS, Mee S, Bigsby RM, Higgins SJ, Sugimura Y. The endocrinology and developmental biology of the prostate. *Endocr Rev* 1987; 8:338-362.
- Cordeiro RS, Scarano WR, Campos SG, Santos FC, Vilamaior PS, Goes RM, Taboga SR. Androgen receptor in the Mongolian gerbil ventral prostate: evaluation during different phases of postnatal development and following androgen blockage. *Micron* 2008; 39:1312-1324.
- Chang SM, Chung LW. Interaction between prostatic fibroblast and epithelial cells in culture: role of androgen. *Endocrinology* 1989; 125: 2719-2727.
- Ohlson N, Bergh A, Stattin P, Wikstrom P. Castration-induced epithelial cell death in human prostate tissue is related to locally reduced IGF-1 levels. *Prostate* 2007; 67:32-40.
- Hayward SW, Cunha GR. The prostate: development and physiology. *Radiol Clin North Am* 2000; 38:1-14.
- Cunha GR, Ricke W, Thomson A, Marker PC, Risbridger G, Hayward SW, Wang YZ, Donjacour AA, Kurita T. Hormonal, cellular, and molecular regulation of normal and neoplastic prostatic development. *J Steroid Biochem Mol Biol* 2004; 92:221-236.
- Sugimura Y, Foster BA, Hom YK, Lipschutz JH, Rubin JS, Finch PW, Aaronson SA, Hayashi N, Kawamura J, Cunha GR. Keratinocyte growth factor (KGF) can replace testosterone in the ductal branching morphogenesis of the rat ventral prostate. *Int J Dev Biol* 1996; 40:941-951.
- Cunha GR, Hayward SW, Dahiya R, Foster BA. Smooth muscle-epithelial interactions in normal and neoplastic prostatic development. *Acta Anat (Basel)* 1996; 155:63-72.
- Laaksonen DE, Niskanen L, Punnonen K, Nyysönen K, Tuomainen TP, Valkonen VP, Salonen JT. The metabolic syndrome and smoking in relation to hypogonadism in middle-aged men: a prospective cohort study. *J Clin Endocrinol Metab* 2005; 90:712-719.
- Zitzmann M. Testosterone deficiency, insulin resistance and the metabolic syndrome. *Nat Rev Endocrinol* 2009; 5:673-681.
- Bobjer J, Naumovska M, Giwercman YL, Giwercman A. High prevalence of androgen deficiency and abnormal lipid profile in infertile men with non-obstructive azoospermia. *Int J Androl* 2012; 35:688-694.

12. Huggins C, Clark PJ. Quantitative studies of prostatic secretion. II. The effect of castration and of estrogen injection on the normal and on the hyperplastic prostate glands of dogs. *J Exp Med* 1940; 72:747–762.
13. Lee C. Physiology of castration-induced regression in rat prostate. *Prog Clin Biol Res* 1981; 75:145–159.
14. Sugimura Y, Cunha GR, Donjacour AA. Morphological and histological study of castration-induced degeneration and androgen-induced regeneration in the mouse prostate. *Biol Reprod* 1986; 34:973–983.
15. Bruchovsky N, Lesser B, Van Doorn E, Craven S. Hormonal effects on cell proliferation in rat prostate. *Vitam Horm* 1975; 33:61–102.
16. English HF, Santen RJ, Isaacs JT. Response of glandular versus basal rat ventral prostatic epithelial cells to androgen withdrawal and replacement. *Prostate* 1987; 11:229–242.
17. Antonioli E, Cardoso AB, Carvalho HF. Effects of long-term castration on the smooth muscle cell phenotype of the rat ventral prostate. *J Androl* 2007; 28:777–783.
18. Shidaifat F, Daradka M, Al-Omari R. Effect of androgen ablation on prostatic cell differentiation in dogs. *Endocr Res* 2004; 30:327–334.
19. Vilamaior PS, Taboga SR, Carvalho HF. Modulation of smooth muscle cell function: morphological evidence for a contractile to synthetic transition in the rat ventral prostate after castration. *Cell Biol Int* 2005; 29: 809–816.
20. Tuohimaa P, Niemi M. The effect of testosterone on cell renewal and mitotic cycles in sex accessory glands of castrated mice. *Acta Endocrinol (Copenh)* 1968; 58:696–704.
21. Morley A, Wright N, Appleton D, Alison M. A cytokinetic analysis of the proliferative response to androgen in the prostatic complex of the castrated mouse. *Biochem Soc Trans* 1973; 1:1081–1084.
22. Leong KG, Wang BE, Johnson L, Gao WQ. Generation of a prostate from a single adult stem cell. *Nature* 2008; 456:804–808.
23. Isaacs JT, Coffey DS. Etiology and disease process of benign prostatic hyperplasia. *Prostate Suppl* 1989; 2:33–50.
24. Isaacs JT. Prostate stem cells and benign prostatic hyperplasia. *Prostate* 2008; 68:1025–1034.
25. Nishi N, Oya H, Matsumoto K, Nakamura T, Miyataka H, Wada F. Changes in gene expression of growth factors and their receptors during castration-induced involution and androgen-induced regrowth of rat prostates. *Prostate* 1996; 28:139–152.
26. Salm SN, Burger PE, Coetzee S, Goto K, Moscatelli D, Wilson EL. TGF- β maintains dormancy of prostatic stem cells in the proximal region of ducts. *J Cell Biol* 2005; 170:81–90.
27. Kyprianou N, Isaacs JT. Expression of transforming growth factor- β in the rat ventral prostate during castration-induced programmed cell death. *Mol Endocrinol* 1989; 3:1515–1522.
28. Wang GM, Kovalenko B, Huang Y, Moscatelli D. Vascular endothelial growth factor and angiopoietin are required for prostate regeneration. *Prostate* 2007; 67:485–499.
29. Donjacour AA, Thomson AA, Cunha GR. FGF-10 plays an essential role in the growth of the fetal prostate. *Dev Biol* 2003; 261:39–54.
30. Lin Y, Wang F. FGF signalling in prostate development, tissue homeostasis and tumorigenesis. *Biosci Rep* 2010 30:285–291.
31. Konno-Takahashi N, Takeuchi T, Nishimatsu H, Kamijo T, Tomita K, Schalken JA, Teshima S, Kitamura T. Engineered FGF-2 expression induces glandular epithelial hyperplasia in the murine prostatic dorsal lobe. *Eur Urol* 2004; 46:126–132.
32. Foster BA, Evangelou A, Gingrich JR, Kaplan PJ, DeMayo F, Greenberg NM. Enforced expression of FGF-7 promotes epithelial hyperplasia whereas a dominant negative FGFR2iib promotes the emergence of neuroendocrine phenotype in prostate glands of transgenic mice. *Differentiation* 2002; 70:624–632.
33. Kaplan-Lefko PJ, Sutherland BW, Evangelou AI, Hadsell DL, Barrios RJ, Foster BA, Demayo F, Greenberg NM. Enforced epithelial expression of IGF-1 causes hyperplastic prostate growth while negative selection is requisite for spontaneous metastogenesis. *Oncogene* 2008; 27:2868–2876.
34. Yoshio Y, Ishii K, Arase S, Hori Y, Nishikawa K, Soga N, Kise H, Arima K, Sugimura Y. Effect of transforming growth factor alpha overexpression on urogenital organ development in mouse. *Differentiation* 80:82–88.
35. Ogura Y, Ishii K, Kanda H, Kanai M, Arima K, Wang Y, Sugimura Y. Bisphenol A induces permanent squamous change in mouse prostatic epithelium. *Differentiation* 2007; 75:745–756.
36. Lipschutz JH, Foster BA, Cunha GR. Differentiation of rat neonatal ventral prostates grown in a serum-free organ culture system. *Prostate* 1997; 32:35–42.
37. Gupta C. Reproductive malformation of the male offspring following maternal exposure to estrogenic chemicals. *Proc Soc Exp Biol Med* 2000; 224:61–68.
38. Sugimura Y, Cunha GR, Donjacour AA. Morphogenesis of ductal networks in the mouse prostate. *Biol Reprod* 1986; 34:961–971.
39. Timms BG, Mohs TJ, Didio LJ. Ductal budding and branching patterns in the developing prostate. *J Urol* 1994; 151:1427–1432.
40. Berquin IM, Min Y, Wu R, Wu H, Chen YQ. Expression signature of the mouse prostate. *J Biol Chem* 2005; 280:36442–36451.
41. Hayward SW. Approaches to modeling stromal-epithelial interactions. *J Urol* 2002; 168:1165–1172.
42. Story MT. Regulation of prostate growth by fibroblast growth factors. *World J Urol* 1995; 13:297–305.
43. Gospodarowicz D, Ferrara N, Schweigerer L, Neufeld G. Structural characterization and biological functions of fibroblast growth factor. *Endocr Rev* 1987; 8:95–114.
44. Story MT, Hopp KA, Molter M, Meier DA. Characteristics of FGF-receptors expressed by stromal and epithelial cells cultured from normal and hyperplastic prostates. *Growth Factors* 1994; 10:269–280.
45. Ishii K, Imamura T, Iguchi K, Arase S, Yoshio Y, Arima K, Hirano K, Sugimura Y. Evidence that androgen-independent stromal growth factor signals promote androgen-insensitive prostate cancer cell growth in vivo. *Endocr Relat Cancer* 2009; 16:415–428.
46. Zhang X, Ibrahim OA, Olsen SK, Umemori H, Mohammadi M, Ornitz DM. Receptor specificity of the fibroblast growth factor family. The complete mammalian FGF family. *J Biol Chem* 2006; 281:15694–15700.
47. Pearson G, Bumeister R, Henry DO, Cobb MH, White MA. Uncoupling Raf1 from MEK1/2 impairs only a subset of cellular responses to Raf activation. *J Biol Chem* 2000; 275:37303–37306.
48. Ghayad SE, Cohen PA. Inhibitors of the PI3K/Akt/mTOR pathway: new hope for breast cancer patients. *Recent Pat Anticancer Drug Discov* 2010; 5:29–57.
49. Hamaguchi A, Tooyama I, Yoshiki T, Kimura H. Demonstration of fibroblast growth factor receptor-1 in human prostate by polymerase chain reaction and immunohistochemistry. *Prostate* 1995; 27:141–147.
50. Saez C, Gonzalez-Baena AC, Japon MA, Giraldez J, Segura DI, Rodriguez-Vallejo JM, Gonzalez-Esteban J, Miranda G, Torrubia F. Expression of basic fibroblast growth factor and its receptors FGFR1 and FGFR2 in human benign prostatic hyperplasia treated with finasteride. *Prostate* 1999; 40:83–88.
51. Bhowmick NA, Chytil A, Plieth D, Gorska AE, Dumont N, Shappell S, Washington MK, Neilson EG, Moses HL. TGF- β signaling in fibroblasts modulates the oncogenic potential of adjacent epithelia. *Science* 2004; 303:848–851.
52. Kurita T, Medina RT, Mills AA, Cunha GR. Role of p63 and basal cells in the prostate. *Development* 2004; 131:4955–4964.
53. Maitland NJ, Frame FM, Polson ES, Lewis JL, Collins AT. Prostate cancer stem cells: do they have a basal or luminal phenotype? *Horm Cancer* 2011; 2:47–61.
54. Maitland NJ, Collins AT. Prostate cancer stem cells: a new target for therapy. *J Clin Oncol* 2008; 26:2862–2870.
55. Cleary KR, Choi HY, Ayala AG. Basal cell hyperplasia of the prostate. *Am J Clin Pathol* 1983; 80:850–854.
56. Dermer GB. Basal cell proliferation in benign prostatic hyperplasia. *Cancer* 1978; 41:1857–1862.
57. Rioux-Leclercq NC, Epstein JI. Unusual morphologic patterns of basal cell hyperplasia of the prostate. *Am J Surg Pathol* 2002; 26:237–243.
58. Shibata Y, Ito K, Suzuki K, Nakano K, Fukabori Y, Suzuki R, Kawabe Y, Honma S, Yamanaka H. Changes in the endocrine environment of the human prostate transition zone with aging: simultaneous quantitative analysis of prostatic sex steroids and comparison with human prostatic histological composition. *Prostate* 2000; 42:45–55.
59. Sugimura Y, Sakurai M, Hayashi N, Yamashita A, Kawamura J. Age-related changes of the prostate gland in the senescence-accelerated mouse. *Prostate* 1994; 24:24–32.
60. Leav I, Schelling KH, Adams JY, Merk FB, Alroy J. Role of canine basal cells in postnatal prostatic development, induction of hyperplasia, and sex hormone-stimulated growth; and the ductal origin of carcinoma. *Prostate* 2001; 47:149–163.
61. Mirosevich J, Bentel JM, Zeps N, Redmond SL, D'Antuono MF, Dawkins HJ. Androgen receptor expression of proliferating basal and luminal cells in adult murine ventral prostate. *J Endocrinol* 1999; 162:341–350.
62. Epstein JI, Netto, GJ. Benign and Malignant Prostate Following Treatment. In: Epstein JI, Netto GJ (eds.), *Biopsy Interpretation of the Prostate*, 4th ed. Philadelphia, PA: Wolters Kluwer Health: Lippincott Williams & Wilkins; 2007: 245–261.
63. Waltregny D, Leav I, Signoretti S, Soung P, Lin D, Merk F, Adams JY, Bhattacharya N, Cirenei N, Loda M. Androgen-driven prostate epithelial cell proliferation and differentiation in vivo involve the regulation of p27. *Mol Endocrinol* 2001; 15:765–782.